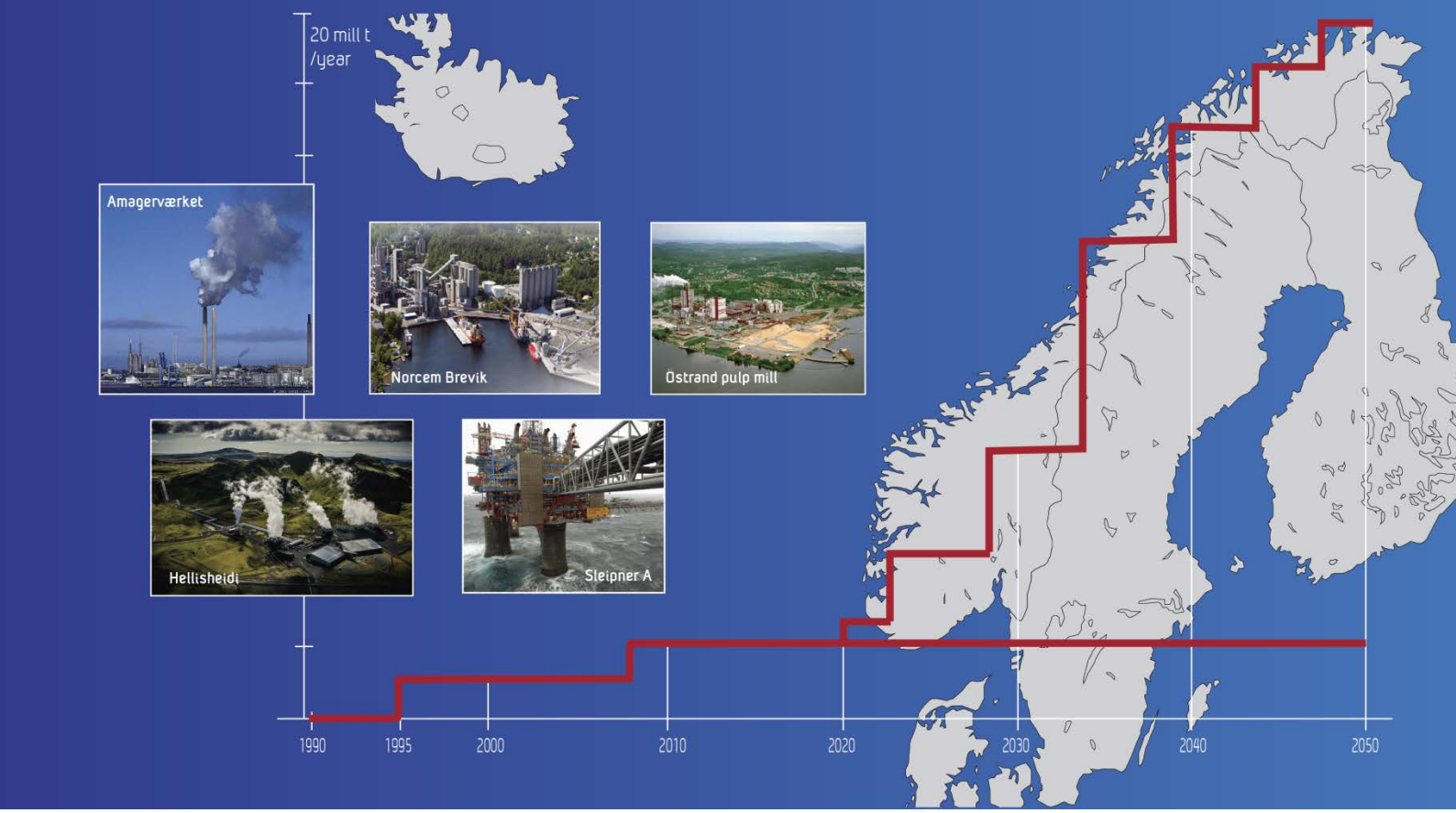

Depressurisation of CO_2-pipelines with volatile gas impurities: Temperature behavior

Eskil Aursand

NORDICCS Technical Report D5.2.1302

December 2013

norden
Top-level Research Initiative

nordiccs
Nordic CCS Competence Centre

CO_2

NORDICCS concept:

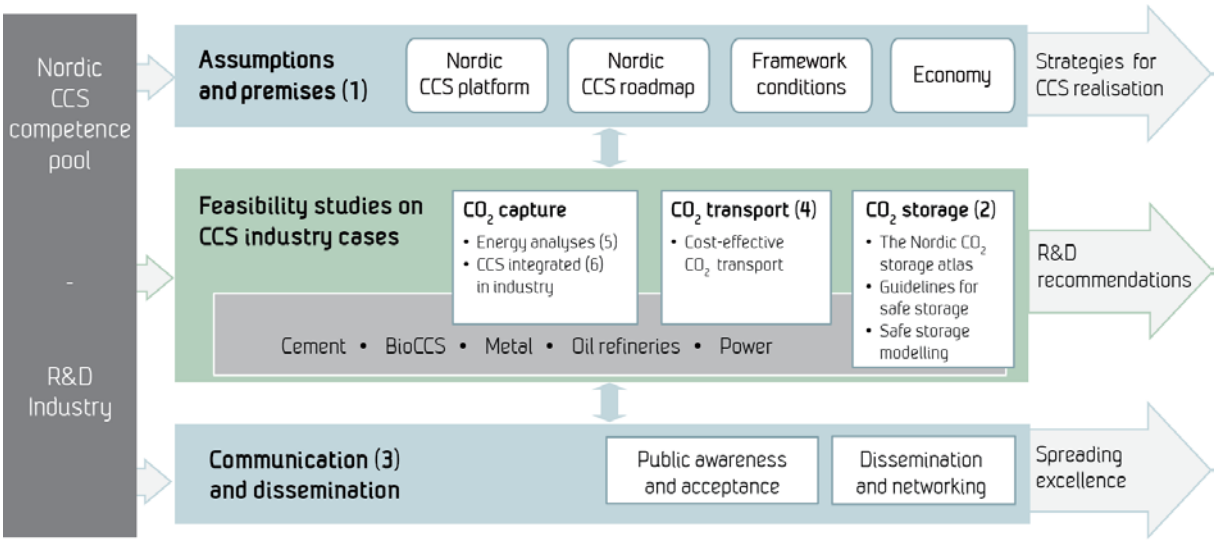

Partners:

VTT · CHALMERS UNIVERSITY OF TECHNOLOGY · IVL Swedish Environmental Research Institute · SGU Sveriges geologiska undersökning Geological Survey of Sweden · GEUS · Orkuveita Reykjavíkur · SINTEF · NTNU · UiO : University of Oslo · tel-tek · UNIVERSITY OF ICELAND · Statoil · GASSCO · NORCEM HEIDELBERGCEMENT Group · VATTENFALL · TECHNOLOGY CENTRE MONGSTAD

Contact: Centre Director Nils A. Røkke • + 47 951 56 181 • Nils.A.Rokke@sintef.no
www.sintef.no/NORDICCS

Summary

This memo is a computational study of the depressurisation of high-pressure pipelines containing CO2 with volatile gas impurities such as N2, CH4 and O2. The focus is on how variables such as kind and amount of impurity affect the temperatures occurring inside the pipeline during depressurisation, and how this compares to the effect of varying the valve size, i.e. the rate of outflow.

The flow was simulated by solving an equilibrium two-fluid two-component 1D flow model, with additional source terms accounting for valve outflow, friction, and wall heat transfer. The results showed that adding volatile gas impurities to pure CO2 slighly reduces the amount of depressurisation temperature-drop, while slightly increasing the speed at which this drop occurs. However, these effects were negligible compared to the effect of slight changes in valve opening radius.

It remains to be seen how other much less volatile impurities such as NOx, SOx, H2S and H2O will affect the temperature drop.

Keywords Fluid dynamics, thermodynamics, impurities, CO_2 transport, depressurisation.

Authors Eskil Aursand, SINTEF Energy Research, Norway, Eskil.Aursand@sintef.no

Date December 2013

About NORDICCS

Nordic CCS Competence Centre, NORDICCS, is a networking platform for increased CCS deployment in the Nordic countries. NORDICCS has 10 research partners and six industry partners, is led by SINTEF Energy Research, and is supported by Nordic Innovation through the Top-level Research Initiative.

Contents

1 Introduction

CO_2 may be transported by pipeline in its liquid or supercritical form. This implies high operating pressures, in the order of 100atm. In such a transport system, depressurisations may occur, either intentionally for shutdown or maintenance, or by accident due to leakage through a damaged section of the pipeline. In the event of such rapid depressurisations/expansions, a fluid will experience a decrease in temperature through the *Joule-Thomson effect*. Additionally, as gas escapes the pipeline, the liquid boils to fill the vacant volume, absorbing the needed latent heat in the process. When these temperature-reducing effects are able to overcome the rate of heat transfer from the surroundings, we have what is called *auto-refrigeration*. Eventually, when all of the gas has vaporised, and most of it has escaped the pipeline, the heat transfer from the surroundings will make the temperature start to increase again.

The above implies that there is a certain minimum temperature occurring in the pipeline at some location and time. It is of interest to predict this lowest temperature for various safety reasons, including ensuring operation above the ductile–brittle transition temperature (DBTT) of the pipeline steel [1], preventing brittle fractures in welds, preventing the formation of ice and hydrates, and generally staying inside the temperature design-specifications of all the equipment involved. Additionally, a high rate of temperature decrease may also be demanding on materials and equipment.

CO_2 transported by pipeline is rarely 100% pure, especially not when coming from capture-processes in a Carbon Capture and Storage (CCS) system. The presence of impurities will influence the thermodynamic behaviour of the fluid compared to pure CO_2 [2], and is thus expected to influence the *auto-refrigeration* when depressurising a pipeline. This work does not cover the effect of all possible impurities, but is limited in scope to N_2, CH_4 and O_2, which represent what will be called the *volatile gas impurities*. By this we mean that their own boiling-points are located at much lower temperatures than the ones reached in these depressurisation events. In their pure form, they would not undergo any phase transition (boiling), but rather be in a gas or supercritical gas-like state throughout the event. This is in contrast to CO_2, which exists as a dense liquid or supercritical liquid-like phase at ordinary operating conditions, and will inevitably begin to boil during such depressurisations.

The effect of impurities should not be studied in isolation, but also compared to the effect of varying other relevant parameters. In this work, the effect of impurity kind and amount on the temperature-behaviour will be compared to the effect of varying the outflow area, *e.g.* the valve opening. In deliberate depressurisation, this is a directly controllable parameter which could be used to offset any negative impurity effects.

The present memo is a computational study, employing multi-phase computational fluid dynamics and thermodynamics. The work relates to the previous NORDICCS deliverable D5.2.1301 by Morin [3], who investigated the possibility of initiating multi-phase flow due to variable flow rates during regular transport to an injection site. In that study, the onset of multi-phase flow was merely noted, and not actually simulated any further. In the depressurisation events studied here, multi-phase flow is inevitable, and its dynamics must be simulated.

2 The model

The depressurisation events are modelled by one-dimensional computational fluid dynamics, accounting for phase transfer and thermodynamic effects, flow of liquid and vapour at different velocities, momentum transfer by friction, heat transfer through pipeline walls, and the loss of mass, momentum and energy though a depressurisation valve.

2.1 Flow equations

The set of governing equations used for the pipeline flow is a two-fluid two-component flow model [4], with additional source terms for valve outflow, friction, and wall heat transfer, with the assumption of instantaneous local mechanical, thermal and chemical equilibrium:

$$\frac{\partial(\rho_g \alpha_g z_{1,g})}{\partial t} + \frac{\partial(\rho_g \alpha_g z_{1,g}) u_g}{\partial x} = -\zeta_{\rho,1,g}, \tag{1a}$$

$$\frac{\partial(\rho_g \alpha_g z_{2,g})}{\partial t} + \frac{\partial(\rho_g \alpha_g z_{2,g}) u_g}{\partial x} = -\zeta_{\rho,2,g}, \tag{1b}$$

$$\frac{\partial(\rho_l \alpha_g z_{1,l})}{\partial t} + \frac{\partial(\rho_l \alpha_l z_{1,l}) u_l}{\partial x} = -\zeta_{\rho,1,l}, \tag{1c}$$

$$\frac{\partial(\rho_l \alpha_g z_{2,l})}{\partial t} + \frac{\partial(\rho_l \alpha_l z_{2,l}) u_l}{\partial x} = -\zeta_{\rho,2,l}, \tag{1d}$$

$$\frac{\partial(\rho_g \alpha_g u_g)}{\partial t} + \frac{\rho_g \alpha_g u_g^2}{\partial x} + \alpha_g \frac{\partial p}{\partial x} + \tau_\mathrm{i} = -\tau_{g,\mathrm{w}} - \tau_{g,l} - \zeta_{\rho u,g}, \tag{1e}$$

$$\frac{\partial(\rho_l \alpha_l u_l)}{\partial t} + \frac{\rho_l \alpha_l u_l^2}{\partial x} + \alpha_l \frac{\partial p}{\partial x} - \tau_\mathrm{i} = -\tau_{l,\mathrm{w}} + \tau_{g,l} - \zeta_{\rho u,l}, \tag{1f}$$

$$\frac{\partial(E_g + E_l)}{\partial t} + \frac{\partial(E_g u_g + \alpha_g u_g p)}{\partial x} + \frac{\partial(E_l u_l + \alpha_l u_l p)}{\partial x} = \zeta_E + Q_\mathrm{w}. \tag{1g}$$

Subscripts g and l refer to gas phase and liquid phase, respectively, while subscripts 1 and 2 indicate chemical components. With k as a generalised phase subscript, ρ_k (kg/m^3) is the density of phase k, while α_k and w_k are the volume and mass fractions of phase k, *i.e.*

$$\alpha_k \equiv \frac{V_k}{V_\mathrm{m}}, \quad w_k \equiv \frac{m_k}{m_\mathrm{m}}, \tag{2}$$

satisfying

$$\sum_k \alpha_k = 1, \quad \sum_k w_k = 1, \tag{3}$$

and are related by

$$\frac{w_k}{\alpha_k} = \frac{\rho_k}{\rho_\mathrm{m}} \tag{4}$$

for any phase k. A subscript m indicates a total for the local mixture. An example is ρ_m, which is the *mixture density* given by

$$\rho_\mathrm{m} = \sum_k \alpha_k \rho_k. \tag{5}$$

Mass fractions of components within phases are given by

$$z_{i,k} \equiv \frac{m_{i,k}}{m_k} \tag{6}$$

satisfying

$$\sum_i z_{i,k} = 1. \tag{7}$$

The variable u_k (m/s) is the velocity of phase k, p (Pa) is the pressure, and E_k (J/m^3) is the total energy per volume of phase k, *i.e.*

$$E_k = \alpha_k \rho_k \left(e_k + u_k^2/2\right), \tag{8}$$

where e_k (J/kg) is the internal energy per mass of phase k. Finally, for the left hand side of (1), we have τ_i (kg(m/s)/(m^{3}s)) , which is the *interfacial momentum exchange*. This may be modelled as [4]

$$\tau_{\mathrm{i}} = -\Delta p_{\mathrm{i}} \frac{\partial \alpha_l}{\partial x}, \tag{9}$$

where Δp_i is the difference between the average pressure and the pressure at the gas-liquid interface, here estimated by the average liquid hydrostatic pressure:

$$\Delta p_{\mathrm{i}} = \frac{1}{2} D \alpha_l \rho_l g. \tag{10}$$

Here g is the gravitational acceleration and D is the pipeline diameter.

The right hand side of (1) contains source terms representing valve leakage (ζ), friction (τ) and wall heat transfer (Q_w). These are described more closely in Sec. 2.2.

The flow model (1) is solved numerically as detailed in Sec. 2.1.2. After the flow model has evolved for one time step, the two phases will generally be out of chemical equilibrium. Therefore, the phase change needed to restore chemical equilibrium is calculated and applied between each time step, using an *equation of state* (Sec. 2.1.1). This is called the *fractional-step* or *time-splitting* method.

The boundary conditions of the one-dimensional flow model represent stationary walls or closed valves. The opening causing the depressurisation event is a valve at the $x = 0$ end of the pipeline, though positioned on the side-wall, perpendicular to the pipeline axis. The initial condition is a spatially constant temperature-pressure state in the pure liquid/dense phase area, with zero velocity.

2.1.1 Thermodynamics and thermophysical properties

The common Soave-Redlich-Kwong (SRK) [5] *cubic* Equation of State (EoS) with Van der Waals mixing rules [6] is used to describe the mixture behaviour.

The instantaneous thermodynamic equilibrium is maintained by performing an *energy-density* flash calculation after each time-step of the numerical solving of (1). This entails using the mixture density and total energy known from the flow equations to calculate new state properties such as pressure, temperature, volume fractions, phase compositions and new phase velocities.

The thermophysical properties such as viscosity and heat conductivity are calculated by the TRAPP corresponding-states model [7, 8].

2.1.2 Numerics

Time-integration of the flow equations (1) is done with the simple Forward Euler method, with the time-step obeying a Courant–Friedrichs–Lewy (CFL) condition

$$\Delta t = C \frac{\Delta x}{\max\left(|c_{\text{mix}} \pm u_k|\right)}, \tag{11}$$

where Δx is the length of a computational cell and c_{mix} is an approximate local speed of sound for the phase mixture, as given by (3.74) in [4]. The function $\max()$ implies finding the maximum value across the pipeline for either phase, at the given time. The condition is set with a constant CFL-number $C = 0.5$.

The spatial numerical scheme is according to the FORCE-flux method [9], extended to handle non–conservative terms [10].

2.2 Source terms

The *source terms* are all the terms on the right hand side of the flow equations (1). The terms representing valve leakage (ζ) are covered in 2.2.1, the term representing wall heat transfer (Q_w) is covered in 2.2.2, and the terms representing friction (τ) are covered in 2.2.3.

2.2.1 Depressurisation valve

The outflow through the valve is assumed to be isentropic, and we must then take into account the phenomenon of *choked flow*, where the fluid velocity at the valve is unable to increase beyond the local speed of sound, no matter the pressure difference [1].

We employ an isentropic homogeneous equilibrium choke model, in which a fluid element flows from inside the pipe at an initial pressure $p_i = p(x)$ to the point of escape at the unknown escape-pressure $p_e(x)$. The escape pressure is within the range $[p_a, p_i]$ if the flow is choked, and equal to p_a if not, with p_a denoting the atmospheric pressure. The initial velocity for the streamline is taken as a weighted average of the gas and liquid velocities at that point in the flow equations:

$$u_0 = \frac{\sum_k \alpha_k \rho_k u_k}{\sum_k \alpha_k \rho_k} \tag{12}$$

Assuming instantaneous equilibrium and equal liquid/vapor velocity in the outflow process, and using the fact that the escape velocity is equal to the local speed of sound when the outflow is choked, we may find the the choke pressure as

$$p_e = \left\{ p \in [p_i, p_a] : \frac{\mathrm{d}}{\mathrm{d}p} \left[\rho_{\text{m}}(p, s_0)^2 \left(\int_{p_i}^{p} \frac{\mathrm{d}p'}{\rho_{\text{m}}(p', s_o)} - \frac{1}{2} u_0^2 \right) \right] = 0 \right\}, \tag{13}$$

i.e. the choke pressure is the pressure at which the expression in the above square parenthesis reaches its minimum value (the integral is negative). The function $\rho_{\text{m}}(p, s)$ is provided by the equation of state. Here s_o is the specific entropy inside the pipeline, *i.e.* corresponding to the

[1] However, increased upstream pressure may increase the local speed of sound, thus allowing faster escape velocity.

current 1D flow variables. If no such maximum can be found, the flow is not choked, and $p_e = p_a$. In the process of finding p_e, ρ_e is also found as the mixture density at the escape point. Once the escape pressure p_e has been found, the escape fluid velocity may be found from Bernoulli's principle as

$$u_e = \sqrt{u_0^2 - 2\int_{p_i}^{p_e} \frac{\mathrm{d}p'}{\rho_\mathrm{m}(p', s_o)}}. \tag{14}$$

The escape velocity found from (14) is interpreted as the absolute speed at the escape point, which may have an x-component and a y-component.

These escape quantities, p_e, ρ_e and u_e, must now somehow be interpreted as source terms in (1). If one considers the integral form of the conservation equations for a homogeneous fluid, one finds with some simplifying assumptions, while ensuring that the specific entropy within the pipeline is conserved, that the source terms are:

$$\begin{aligned}
\zeta_\rho &= \left(-\frac{\rho_e u_{y,e} A_e}{V_\mathrm{cell}}\right), \\
\zeta_{\rho u} &= \left(-\frac{\rho_e u_{y,e} A_e}{V_\mathrm{cell}}\right) \cdot u_0, \\
\zeta_E &= \left(-\frac{\rho_e u_{y,e} A_e}{V_\mathrm{cell}}\right) \cdot \left(e + \frac{p}{\rho} + \frac{1}{2}u_x^2\right),
\end{aligned} \tag{15}$$

where A_e is the valve opening area, V_cell is the volume of the computational cell containing the valve, and the y-component of the escape velocity is given by

$$u_{y,e} = \sqrt{u_e^2 - u_0^2}. \tag{16}$$

In order to use this in (1), the source terms for mass and momentum have to be distributed between the multiple mass and momentum equations. The mass source term is distributed among the first source terms in (1) according to

$$\frac{\zeta_{\rho,i,k}}{\zeta_\rho} = \frac{m_{i,k}}{m_\mathrm{m}} = w_k \cdot z_{i,k}, \tag{17}$$

i.e. weighted by the ratio of mass of component i in phase k to the total mass, as given by the state in the pipeline cell. Similarly, the momentum source term is distributed according to

$$\frac{\zeta_{\rho u,k}}{\zeta_{\rho u}} = \frac{\alpha_k \rho_k u_k}{\sum_k \alpha_k \rho_k u_k}, \tag{18}$$

i.e. weighted by the ratio of momentum in the given phase to the total momentum.

The energy source term ζ_E does not need to be distributed, as there is only one equation for energy conservation.

2.2.2 Wall heat transfer

The heat transfer model is completely axisymmetric, with a shell representing the pipeline wall inside a shell representing the soil around the buried pipeline. The soil shell is an approximation to the real situation, which is a flat soil surface some distance above and essentially infinite lengths of soil in other directions.

The heat transfer between the fluid and the pipeline wall is calculated through

$$\mathrm{q} = h_i(T_\mathrm{w} - T) \tag{19}$$

where $q(\mathrm{W/m^2})$ is the amount of heat transfer rate into the fluid per area of pipeline wall, and $T_\mathrm{w}(\mathrm{K})$ is the pipeline inner wall temperature. The *inner heat transfer coefficient*, $h_i(\mathrm{W/(m^2K)})$, is calculated based on the Colburn correlation [11], using volume-averaged properties as input.

The source term $Q_\mathrm{w}(\mathrm{W/m^3})$ in (1g) is the heat transfer rate per volume of fluid, *i.e.*

$$Q_\mathrm{w} = \frac{A_\mathrm{w}}{V_\mathrm{cell}} q = \frac{2\pi r_i \mathrm{d}x}{\pi r_i^2 \mathrm{d}x} q = \frac{2}{r_i} q = \frac{2}{r_i} h_i(T_\mathrm{w} - T) \tag{20}$$

where A_e is the wall heat transfer area, and r_i is the inner radius of the pipeline.

The temperature profile at the inside of the solids (pipeline metal and soil) is calculated transiently by integrating the axially symmetric heat conduction equation from the temperature profile in the previous time step. The heat transfer between air and soil is calculated from a constant *outside heat transfer coefficient*.

Note that only radial heat conduction is included, *i.e.* there is no conduction along the pipeline axis, between computational cells. However, *convective* axial heat transfer is included in (1).

2.2.3 Friction momentum exchange

This section briefly explains the calculation of the friction terms in the flow equations (1), which include $\tau_{g,\mathrm{w}}$ (gas-to-wall momentum transfer), $\tau_{l,\mathrm{w}}$ (liquid-to-wall momentum transfer), and $\tau_{g,l}$ (gas-to-liquid momentum transfer).

Where the flow is single-phase, $\tau_{g,l} = 0$, and $\tau_{k,\mathrm{w}}$ is calculated from the Darcy-Weisbach equation. The Haaland friction factor [12] with a relative roughness factor of 5×10^{-5} is used where the flow is turbulent, and a friction factor of $64/\mathrm{Re}$ is used where the flow is laminar.

Where there is two-phase flow, the three friction terms are calculated from the Spedding & Hand two-fluid friction model [13].

3 Simulation cases

The cases simulated in this work is the depressurisation/emptying of a 10 km pipeline containing a binary mixture of CO_2 with an impurity. The pipeline section has been closed off at the ends in the axial direction, and the emptying is performed by opening a perpendicular valve close to one end. The full set of case parameters common to all simulations are shown in Tab. 1. The initial state of the fluid is as listed in Tab. 2.

The impurities studied here are N_2, CH_4 and O_2. These are all considerably more volatile gases than CO_2. The temperature ranges encountered in the simulations in this work are all well above the critical temperatures of the impurities alone, while below the critical temperature of CO_2 (see Tab. 3). Note that when impurity concentrations are shown without further explanation, they are implicitly *molar fractions*. The corresponding *mass fractions* will depend on the molar masses of the substances involved (see Tab. 4).

4 Grid sensitivity test

Numerical solutions to differential equations should be submitted to *grid sensitivity tests* in order to find the grid density which gives sufficiently accurate calculations. A grid sensitivity test was performed with the test composition 95% CO_2 / 5% N_2. The tests started with 100 computational cells. Then the number of cells was repeatedly multiplied by 3 to make sure all grids have a subset of their cell centres at the same locations as the 100-cell grid. The error-measure is the average of the error at these common points, relative to the solution found with a 24300-cell reference grid. In order to make this test computationally feasible, the errors are evaluated as soon as 10 s into the depressurisation event. The cells to the left of 250 m are not included in the error measure, as the presence of the valve disturbs the convergence.

The results of the convergence test is shown in Fig. 1. While it appears that the numerical error can be made arbitrarily small by increasing the number of cells, a compromise must be found between keeping the numerical error low, and keeping the computational time feasible. In the rest of this work, a domain of 250 grid cells will be used. Using Fig. 1a and 1b, this would imply a numerical error in the area of 1-2% for the temperature and pressure. Increasing the grid density beyond this seems unnecessary, as the model-errors are likely at least this high, and as the computational time for the numerous simulations needs to be kept reasonable.

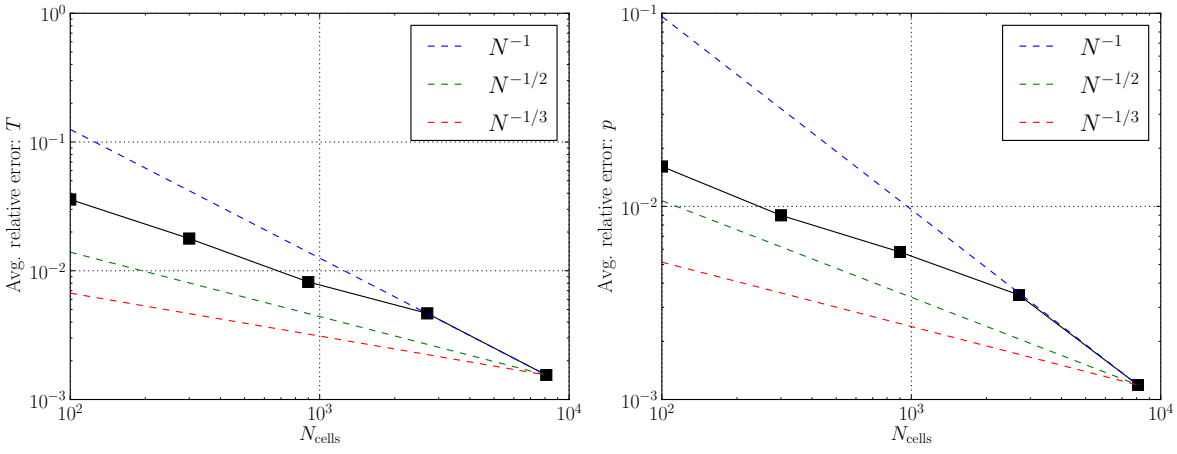

(a) (b)

Figure 1: Logarithmic plots of the average relative errors in (a) temperature and (b) pressure against the number of computational cells. Dashed lines show various power-laws, for comparison.

Table 1: Properties of the pipeline and its surroundings, common to all cases.

Parameter	Value	Used in model(s)
Pipeline geometry		
Pipeline length	10 km	Flow equations
Valve position	≈ 0 m	Flow equations, Valve
Pipeline inner diameter	20 cm	Valve, Friction
Pipeline wall thickness	1.0 cm	Wall heat transfer
Pipeline material properties		
Pipeline thermal conductivity	45 W/(mK)	Wall heat transfer
Pipeline density	7850 kg/m^3	Wall heat transfer
Pipeline specific heat capacity	470 J/(kgK)	Wall heat transfer
Surroundings		
Soil thermal conductivity	2.6 W/(mK)	Wall heat transfer
Soil density	1800 kg/m^3	Wall heat transfer
Soil specific heat capacity	1000 J/(kgK)	Wall heat transfer
Soil radius outside pipeline	1.0 m	Wall heat transfer
Outside heat transfer coefficient	4.0 W/(m^2 K)	Wall heat transfer
Outside temperature	10 °C	Wall heat transfer
Outside pressure	1 atm	Valve

Table 2: Initial conditions common to all cases.

Parameter	Value
Initial pressure	100 bar
Initial temperature	10 °C
Initial velocity	0 m/s

Table 3: Triple- and critical-point properties of CO_2 and the impurities used in this work.

	CO_2	N_2	CH_4	O_2
T_{triple} (°C)	-57	-210	-182	-219
p_{triple} (bar)	5	0.1	0.1	0.002
T_{crit} (°C)	31	-147	-83	-119
p_{crit} (bar)	74	34	46	50

Table 4: The mass fractions of different impurities in a binary mixture with CO_2, at given impurity molar fractions.

mol%	N_2	CH_4	O_2
1%	0.639%	0.367%	0.729%
2%	1.283%	0.738%	1.462%
3%	1.931%	1.115%	2.199%
4%	2.584%	1.496%	2.940%
5%	3.242%	1.882%	3.686%

5 Results

The model described in Sec. 2 was run on a set of cases as described in Sec. 3. First, the general qualitative behaviour of these cases is described Sec 5.1. Then, two kinds of parameter variations are performed:

- Varying the kind and amount of impurity, while keeping the valve area at a constant 50 cm^2 (Sec. 5.2).
- Varying the valve area, while keeping the composition at 2 mol% N_2 (Sec. 5.3).

The focus was on how these parameters influenced the temperatures reached in the pipeline during the depressurisation.

5.1 General behaviour

The qualitative behaviour of these simulations with different kinds and amounts of volatile gas impurities is quite similar. In this section, this behaviour will be outlined using the case of 5 mol% N_2 and a 50 cm^2 valve opening.

Figure 2a shows the temperature-pressure (TP) evolution in this case, close to the valve at one end, and at the opposite end. These lines are shown together with a map of the two-phase region, *i.e.* the *phase envelope*. For each line, the marked points show, in chronological order, the initial state, the onset of boiling, the point of reaching 40 bar, the end of boiling, and the point of reaching within 1% of 1 atm. The temperature, gas volume fraction and average composition profiles along the pipeline at a selection of these times are shown in Fig. 2b, 2c and 2d, respectively.

Some important phases/events in this case should be mentioned:

- The opening of the valve at $x = 0$ causes a sudden local pressure drop, and initiates a pressure wave. This pressure wave carries the first information about the valve-opening event through the pipeline, and its front moves at the initial speed of sound in the mixture, about 450 m/s. After about 20 s, the wave reaches the other end, and the entire 10 km pipeline "knows" about the event.
- After about 20 s the TP-state in the pipeline at $x \approx 0$ reaches the bubble line, and starts to boil. Note that the actual outflow stream through the valve has involved boiling since the beginning, but this event signifies the onset of boiling inside the pipeline.
- After approximately 47 min the first case of a local pure gas state occurs, at $x \approx 0$. The region of pure gas proceeds to spread smoothly towards the other end of the pipeline, until all liquid is gone at approximately 65 min.
- After approximately 2 h, the entire 10 km pipeline reaches atmospheric pressure. At this point, the gas is still at the reduced temperature of approximately 0 °C, and continues to approach the ambient 10 °C for some hours.

Note that the phase envelope in Fig. 2a corresponds to the initial 5% composition, while the actual average composition[2] varies in time and space as the simulations proceeds. The variations

[2] *Average composition* means composition in a pipeline section as a whole, *i.e.* the sum of moles of the given component over all present phases, relative to the total number of moles of any kind present in the same volume.

in average composition is due to the fact that in regions of two-phase states, the gas phase and the liquid phase will have different compositions from the local average composition. In this case, the gas phase will be richer in the volatile impurity, while the liquid phase will be richer in CO_2. Since the model in (1) allows for different velocities of the phases, components can be transported in rates out of proportion with its fraction of the average composition, leading to inhomogeneous average composition.

However, as seen in Fig. 2a, the TP-paths still align quite well with the initial phase envelope. The match of the bubble line is due to the fact that the flow has been single-phase liquid so far, and in single phase the average composition is equal to the phase composition, making a component separation impossible. At the time of dew line encounter, the average compositions have changed considerably, but the correspondence is still good because the low-temperature parts of the dew line are quite composition-independent in these mixtures (as seen later in Fig 3 b,d,f).

In this case, the ouflow has an impurity concentration higher than the initial 5%. This is because the outflow occurs where the valve is ($x = 0$), which is a region of high gas fraction due to the pressure drop. Since the gas is impurity rich, more impurity is lost through the valve compared to the case of simply removing mixture of the initial average composition. This is seen in Fig. 2d, where the average mol% N_2 drops from 5% to less than 2.5% before the depressurisation is complete. Note also how the mol% N_2 is initially increased from the initial value at the valve, due to the rapid transport of N_2-rich gas towards the valve, compared to the liquid velocity.

5.2 Effect of impurities

Simulations were performed on the depressurisation of a pipeline containing CO_2 with N_2, CH_4 or O_2 as the impurity. A valve area of $50\,cm^2$ was used. The results, presented in Fig. 3, focus on the evolution of the thermodynamic state in the computational cell containing the valve, which is where the lowest temperatures are reached. From these results, one may find the lowest temperature occurring throughout a simulation. How this value depends on impurity kind and fraction is shown in Fig. 4.

5.3 Effect of valve opening

Simulations were performed on the depressurisation of a pipeline containing 2 mol% N_2, with a variable valve opening area. The results are presented in Fig. 5 and 6, similarly focusing on the thermodynamic state of the cell containing the valve. Note in Fig. 5a how there are some numerical instabilities in the later parts of the simulations when the valve area becomes very large. These may likely be removed by reducing the cell size and time steps further.

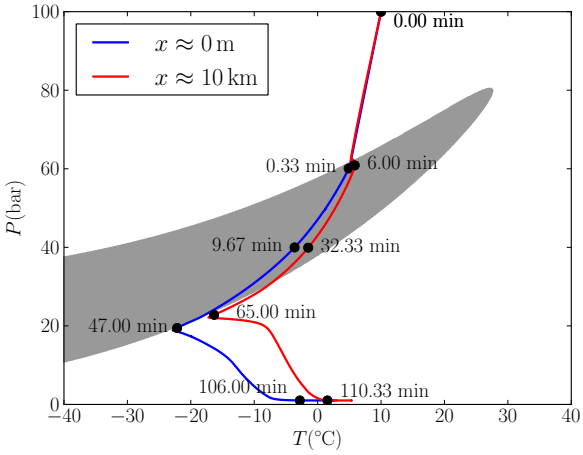

(a) Temperature-pressure evolution

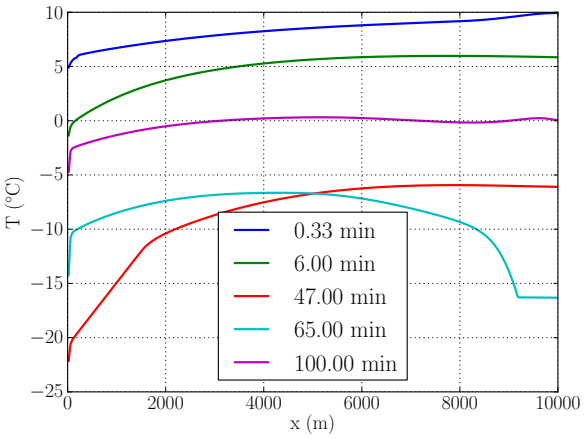

(b) Temperature

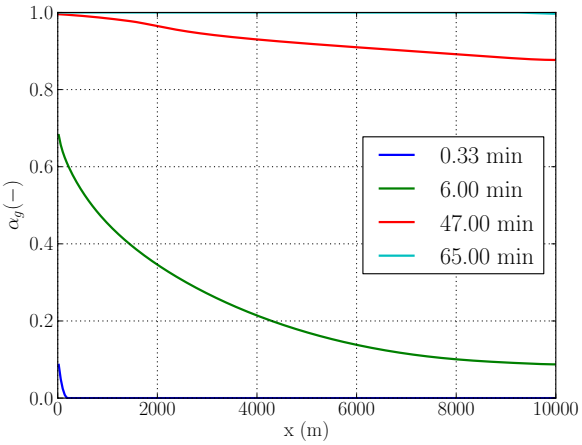

(c) Gas volume fraction

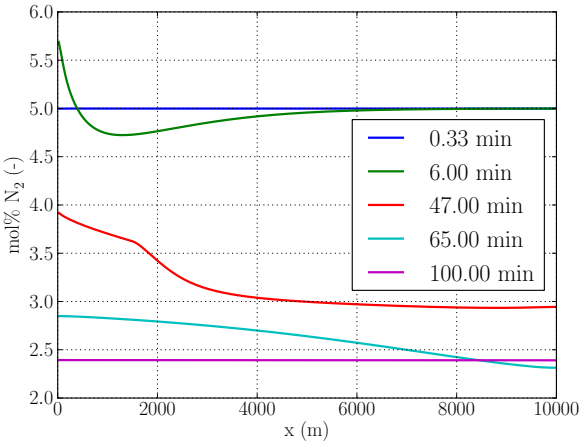

(d) Overall impurity molar fraction

Figure 2: A closer look at the case of 5 mol% N_2 and a 50 cm^2 valve opening. The first figure (a) shows the temperature-pressure evolution at the pipeline end by the valve (blue line) and at the opposite end of the valve (red line), together with the phase envelope corresponding to the initial composition. The temperature, gas volume fraction and average composition profiles along the pipeline at a selection of the times in (a) are shown in (b), (c) and (d), respectively.

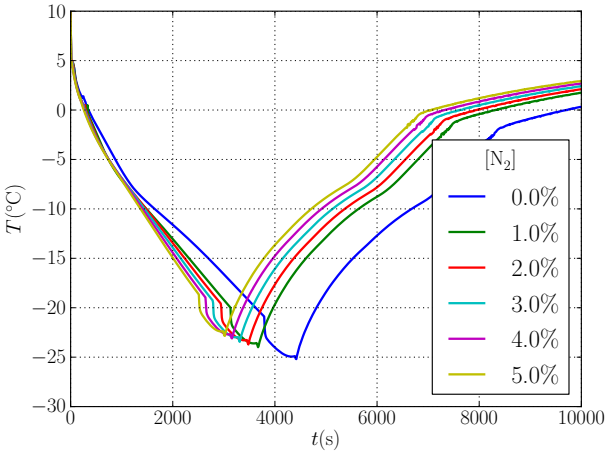

(a) N_2: Temperature *vs.* time at valve

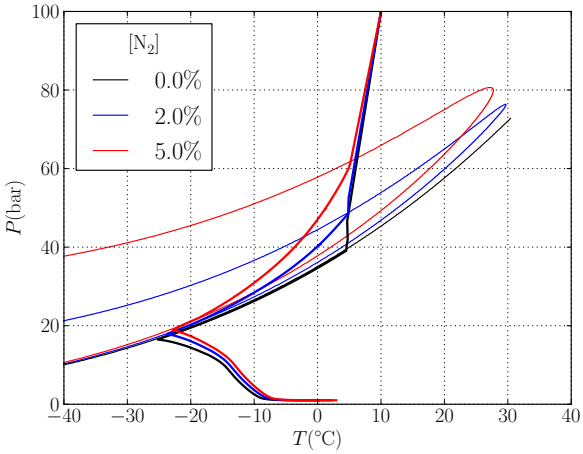

(b) N_2: TP evolution at valve

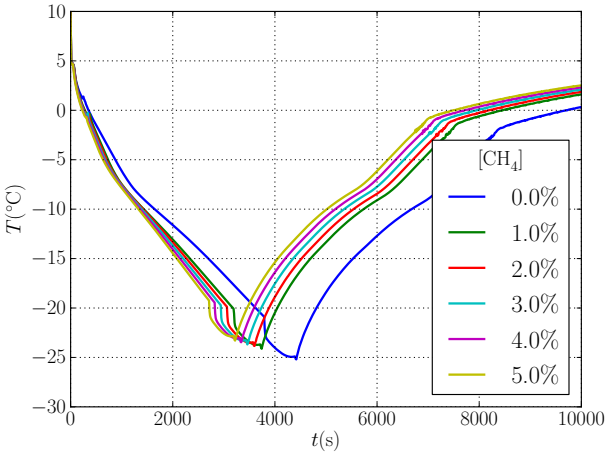

(c) CH_4: Temperature *vs.* time at valve

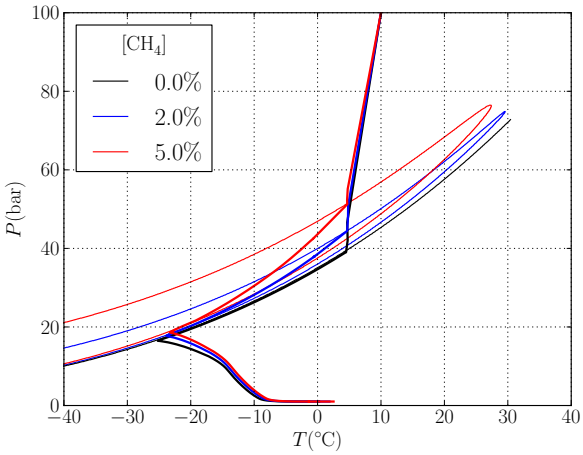

(d) CH_4: TP evolution at valve

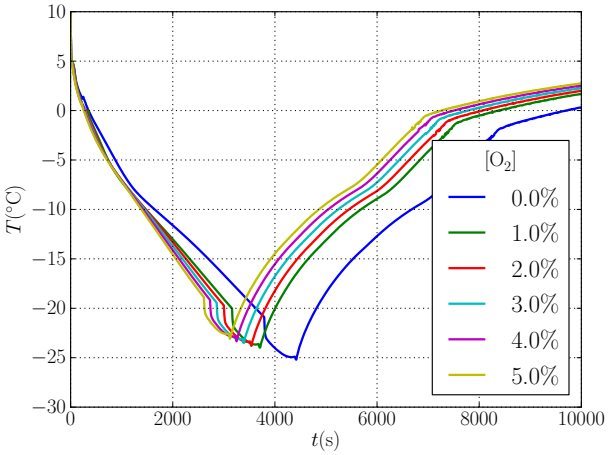

(e) O_2: Temperature *vs.* time at valve

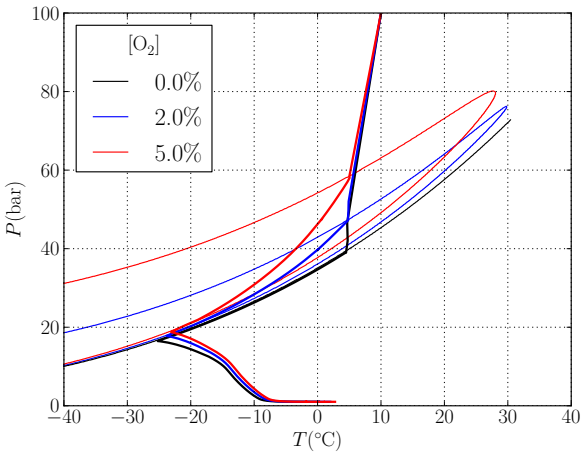

(f) O_2: TP evolution at valve

Figure 3: Results from the depressurisation of a pipeline containing CO_2 with N_2 (a,b), CH_4 (c,d) or O_2 (e,f), at varying impurity molar fraction. On the left, the temperature in the cell with the valve is plotted against time. On the right, the temperature-pressure evolution of the cell with the valve is shown. The phase envelope for the initial composition is also shown, corresponding to the simulation result of the same colour.

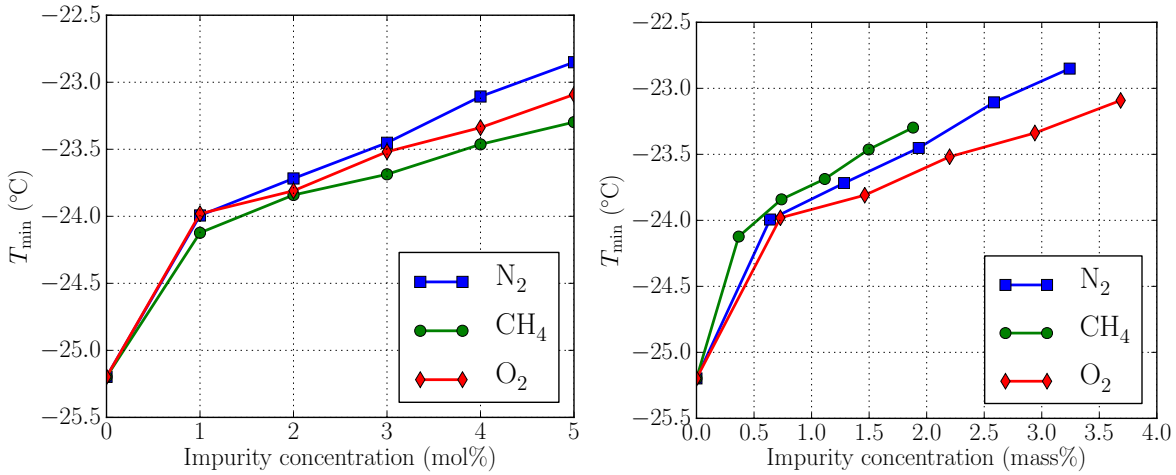

(a) (b)

Figure 4: Results from the simulations shown in Fig. 3, with focus on the lowest temperature achieved in the pipeline. The dependency of this temperature on (a) molar and (b) mass impurity fraction is plotted for each impurity.

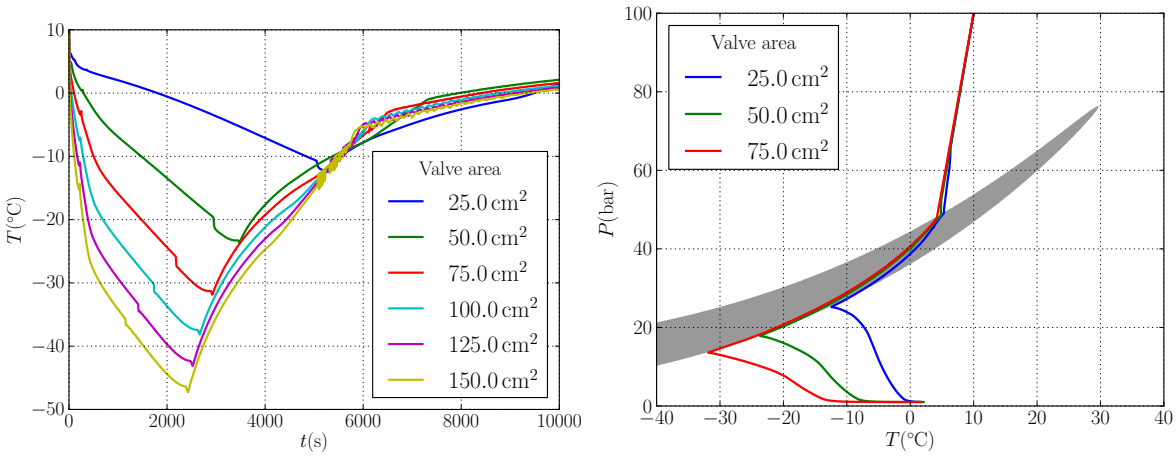

(a) (b)

Figure 5: Results from the depressurisation of a pipeline containing CO_2 with 2 mol% N_2, with varying valve opening area. The temperature of the cell with the valve is plotted against time in (a), while the temperature-pressure evolution of the same cell is shown in (b), together with the phase envelope corresponding to the initial composition.

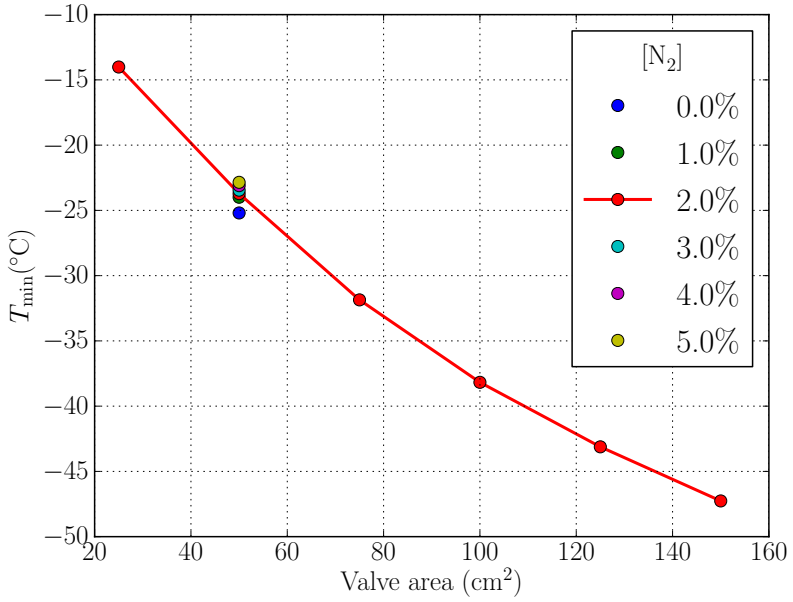

Figure 6: The line shows the effect of valve opening area on the lowest temperature achieved in the pipeline, with a 2 mol% N_2 mixture. For comparison, single dots show the results for N_2 at 50 cm^2 with variable impurity fraction.

6 Discussion

With regards to the effect of impurities, from studying the results presented in Fig. 3 and 4 one may claim the following:

- The presence of volatile gas impurities *increases* the lowest temperature reached, but to a very small degree (no more than about 2 °C for molar fractions up to 5%).
- The presence of volatile gas impurities increases the rate of the temperature drop slightly.
- It does not seem to matter which of these impurities is present, especially when comparing them by molar fraction.

With regards to the effect of valve opening area, the results in Fig. 5 imply that:

- Increasing the valve area decreases the lowest temperature reached dramatically. In the region of 50 cm^2, the lowest temperature decreases by approximately 10 °C per centimetre of increased radius of a circular opening.
- Increasing the valve area also dramatically increases the rate of temperature drop.

Altogether it appears that the effect of the volatile gas impurities on the temperature drop is negligible compared to the effect of reasonable variations in valve opening area. The two effects are compared in Fig. 6 for the case of N_2 as the impurity.

7 Conclusions

It appears that the presence of volatile gas impurities, here exemplified by N_2, CH_4 and O_2, does *not* make the risk of reaching too low temperatures more severe during CO_2 pipeline depressurisation. On the contrary, their presence seems to slightly increase the lowest temperature experienced in the pipeline. However, their presence increases the rate of temperature decrease slightly. Additionally, it seems that the depressurisation behaviour changes very little when switching between different kinds of volatile gas impurities.

On the other hand, the valve opening appears to have a major effect on the temperatures reached and the rate at which it decreases, with a larger opening causing lower temperatures and faster drop. In the case of intentional and controlled depressurisation, this implies that any worries regarding an increased magnitude or rate of temperature drop due to other parameters may likely be remedied by a slight decrease in the valve opening, if an increase in total time required to empty the pipeline is acceptable.

Note that this does *not* mean that the presence if volatile gas impurities should be ignored. These imputities significantly enlarge the two-phase area in temperature-pressure space, compared to pure CO_2. This means that the risk of initiating two-phase flow during pipeline operation is increased, as indicated in [3], something which may introduce many other challenges and potential problems in addition to temperature drops.

7.1 Suggestions for further work

Keep in mind that this work only covered a sub-set of the possible impurities which may be present in CO_2 from capture processes. It remains to be seen how other much less volatile impurities such as NO_x, SO_x, H_2S and H_2O will affect the temperature drop. The latter two are of particular interest, since they may separate into their own liquid phase in addition to a CO_2-rich liquid phase, introducing severe corrosion issues. These impurities present considerable additional challenges for the thermodynamic algorithms, an issue which must be resolved before a similar study of two-phase flow can be performed with such mixtures. Further work could also attempt to study mixtures of more than two components at once, or attempt to vary other parameters than composition and valve, such as initial pressure, pipeline radius, heat transfer conditions, *etc.*

References

[1] J. Capelle et al. "Design based on ductile–brittle transition temperature for API 5L X65 steel used for dense CO2 transport". In: *Engineering Fracture Mechanics* 110.0 (2013), pp. 270 –280.

[2] P. Aursand et al. "Pipeline transport of CO2 mixtures: Models for transient simulation". In: *International Journal of Greenhouse Gas Control* 15.0 (2013), pp. 174 –185.

[3] Alexandre Morin. *Dynamic flow of CO2 in pipelines: Sensitivity to impurities*. NORDICCS Memo D5.2.1301. SINTEF Energy Research, 2013.

[4] Pedro José Martínez Ferrer, Tore Flåtten, and Svend Tollak Munkejord. "On the effect of temperature and velocity relaxation in two-phase flow models". In: *ESAIM: Mathematical Modelling and Numerical Analysis* 46.02 (2012), pp. 411–442.

[5] Giorgio Soave. "Equilibrium constants from a modified Redlich-Kwong equation of state". In: *Chemical engineering science* 27.6 (1972), pp. 1197–1203.

[6] TY Kwak and GA Mansoori. "Van der Waals mixing rules for cubic equations of state. Applications for supercritical fluid extraction modelling". In: *Chemical engineering science* 41.5 (1986), pp. 1303–1309.

[7] J. F. Ely and H. J. M. Hanley. "Prediction of Transport Properties. 1. Viscosity of fluids and mixtures". In: *Industrial & Engineering Chemistry Fundamentals* 20.4 (Nov. 1981), pp. 323–332.

[8] J. F. Ely and H. J. M. Hanley. "Prediction of Transport Properties. 2. Thermal conductivity of pure fluids and mixtures". In: *Industrial & Engineering Chemistry Fundamentals* 22.1 (Feb. 1983), pp. 90–97.

[9] Eleuterio F. Toro. *Riemann solvers and numerical methods for fluid dynamics*. Second. Berlin: Springer-Verlag, 1999. ISBN: 3-540-65966-8.

[10] Svend Tollak Munkejord, Steinar Evje, and Tore FlÅtten. "A MUSTA scheme for a non-conservative two-fluid model". In: *SIAM Journal on Scientific Computing* 31.4 (2009), pp. 2587–2622.

[11] Adrian Bejan. *Heat Transfer*. New York: John Wiley & Sons, Inc., 1993. ISBN: 0-471-50290-1.

[12] Skjalg E. Haaland. "Simple and explicit formulas for the friction factor in turbulent pipe flow". In: *Journal of Fluids Engineering – Transactions of the ASME* 105 (1983), pp. 89–90.

[13] PL Spedding and NP Hand. "Prediction in stratified gas-liquid co-current flow in horizontal pipelines". In: *International journal of heat and mass transfer* 40.8 (1997), pp. 1923–1935.